


ARTICLE



Method for combining valves with symmetric and asymmetric cylinders for hydraulic systems

Mário C. Destro and Victor J. De Negri 

LASHIP, Department of Mechanical Engineering, Federal University of Santa Catarina, Florianópolis, SC, Brazil

ABSTRACT

Electro-hydraulic position control systems are widely applied in several fields. The valve and cylinder configuration and the dimensioning of these systems is dependent on the requested transient response and the load profile. One of the primary factors in this regards is the selection of an asymmetric or symmetric cylinder, considering issues such as the area available for installation and the asymmetry of the external loading. According to the classical literature, the valve control orifice areas must be matched with the cylinder areas to ensure balanced pressure variation in the cylinder chambers. Moreover, considering that several real applications use non-matched components, it is evident that, depending on the system parameters and load characteristics, good performance can be obtained with this system configuration. Based on non-linear dynamic modelling and experimental results, the transient instants when cavitation or high pressure peaks can occur are determined. Subsequently, a set of equations establishing the relationship between the valve control orifice ratio and cylinder area ratio are derived. A method for determining the valve characteristics, based on parameters such as moved mass, external load force and cylinder asymmetry, is presented. The results obtained are also valid for speed control in open or closed loop system.

ARTICLE HISTORY

Received 21 November 2017
Accepted 23 May 2018

KEYWORDS

Electro-hydraulic system;
hydraulic circuit design;
component sizing;
asymmetric and symmetric
cylinder; proportional valve

Introduction

Electro-hydraulic position control systems are widely applied in several fields, including aerospace, vehicles, construction machinery, simulators, machine tools and power plants and encompassing industrial and mobile applications. The most conventional system architecture makes use of an electrically-modulated 4/3 hydraulic control valve (EHV), such as a servo-valve or directional proportional valve, controlling a cylinder in a closed-loop system.

Despite the extensive use of valve-controlled positioning systems, the choice of the component configuration and dimensioning remains a challenge. Each application has specific static and dynamic requirements that must be fulfilled under loadings that are often not precisely known by the system designer. Dynamic simulation can be applied for choosing the valve and cylinder characteristics; however, several component parameters must be set a priori as well as the detailed mathematical model. Saad and Liermann (2015) propose the use of inverse simulation for designing and optimising hydraulic positioning systems. It is an alternative to be using batch dynamic simulation to find the best component characteristics and sizes.

On the other hand, an analytical method for sizing the hydraulic cylinder and the servovalve or directional proportional valve was developed, as presented in Furst (2001), De Negri *et al.* (2008), and Muraro *et al.* (2013).

The valve is dimensioned taking into account the desired transient response of the system, since under steady state conditions no flow rate is required. This method considers the necessity to match a symmetric valve with a symmetric cylinder or an asymmetric valve with an asymmetric cylinder. These configurations result in a balanced pressure variation in the cylinder chambers, avoiding the occurrence of cavitation or pressure peaks.

In many cases, the use of a single rod cylinder is a convenient approach to reducing the physical area occupied or considering the asymmetry of the external loading. In this case, a symmetric directional valve would not be used, as reported in several studies (Viersma 1980, Lei *et al.* 2010, and Guo *et al.* 2014). Nevertheless, in industrial and academic circuits, good performance has been achieved by combining valves with symmetric metering orifices and asymmetric cylinders (Kim and Lee 2006, Sun *et al.* 2006, Detiček and Župerl 2011). Therefore, it can be concluded that, depending on the system parameters and load characteristics, non-matched assemblies of valve and cylinder do not cause significant pressure variations inside the hydraulic lines.

In this context, this paper presents an analysis of the transient conditions when cavitation or pressure peaks can occur. Subsequently, a mathematical model describing the critical pressure conditions is derived,

which requires simple system characteristics such as cylinder areas, moved mass, external load force, and maximum desired acceleration. The final achievement is a method for determining the valve requested characteristics. Despite of the system modelled in this paper is for position control, the proposed method is also valid for speed control using a directional proportional valve in an open or closed-loop system.

The final results presented in this paper can be applied in different fields. For example, hydraulic speed governors in hydroelectric power plants typically use two or more asymmetric cylinders applying force in opposite or the same direction. In the last case they operate as an unique asymmetric cylinder. Dam gates and water inlet valves are also controlled by single rod cylinders. Mobile machines typically demand load movements with controlled speed using single rod cylinders: Telescopic boom in cranes, dump trucks, boom and bucket in earthmoving machines and platforms in harvesting machines are some examples. The reduced space occupied by this cylinder design is also convenient in industrial machines such as hydraulic press brakes and injection moulding machines, among others.

Electro-hydraulic positioning system

The position control system under analysis is shown in Figure 1, where an electrically modulated hydraulic control valve (EHV) drives a hydraulic cylinder in closed-loop control. The reference position is defined by the voltage U_r and U_s corresponds to the piston position. The error signal from the controller is the input voltage to the valve (U_c). The supply and return pressures are assumed constant.

As previously mentioned, single rod cylinders are preferred, considering their lower cost, simpler construction, and the smaller space occupied compared with double-rod cylinders, unless the two sides of the rod are required to attach an external load or other devices. The presence or not of symmetry in the resulting hydraulic force also determines the type of

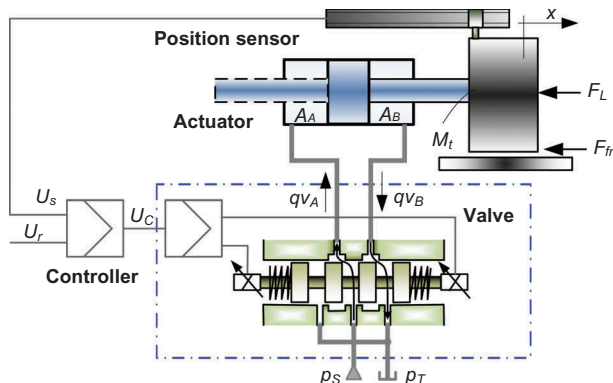


Figure 1. Electro-hydraulic positioning system.

cylinder. Therefore, the cylinder type and dimensioning will determine its area ratio, expressed as:

$$r_A = \frac{A_A}{A_B}, \quad (1)$$

where A_A and A_B are the cylinder chamber areas.

In its turn, both symmetric and asymmetric EHV's are also provided by hydraulic manufacturers. Symmetric EHV's have equal metering orifice areas in all flow paths, such that the flow rates at valve ports A and B will be equal under the same pressure drops. On the other hand, for asymmetric valves, the metering orifice areas in P to A and A to T are higher than in P to B and B to T. Consequently, the flow rate at working port A will be higher than at port B. An usual way to manufacture valves is machining spherical notches at the spool lands as illustrated in Figure 2.

The metering orifice area is a geometric characteristic which is not given on valve datasheets. Instead, an EHV can be characterised by the flow coefficient (De Negri *et al.* 2008, Johnson 1996), which is calculated from the valve flow rate at the nominal input signal ($qv_n @ U_{Cn}$) and measured at a specified pressure drop (Δp_n):

$$Kv = \frac{qv_n}{\sqrt{\Delta p_n}} = c_d w \sqrt{2/\rho} \quad (2)$$

As shown in this expression, the flow coefficient can be also correlated with the discharge coefficient (c_d), fluid density (ρ) and orifice width (w) according to Bernoulli's equation. Equations (4)–(7) below use flow coefficients determined for each valve working port (Kv_A and Kv_B), which means they were determined for pressure drops through P to A or A to T and P to B or B to T, respectively.

Therefore, a flow coefficient ratio, which is equivalent to a valve metering orifice area ratio, can be represented by:

$$r_V = \frac{Kv_A}{Kv_B} \quad (3)$$

Most off-the-shelf servovalves and directional proportional valves are symmetric ($r_V = 1$). However, some types of valves are produced with an asymmetric

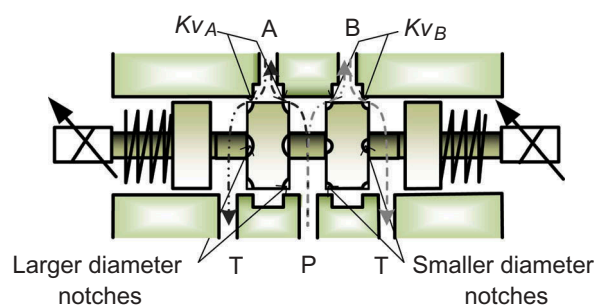


Figure 2. Flow coefficients in an asymmetric valve.

geometry, having typical flow coefficient ratios of 1.33 (4:3) and 2 (2:1).

In the next chapters, theoretical and experimental results are discussed in order to identify critical operating conditions for each combination of cylinder and valve. Based on these results, an analytical model for calculating the range of valve flow coefficient ratios that results in a feasible system is proposed. Cylinder areas, load mass, external load force and the maximum expected acceleration must be taken into account to carry out this calculation.

Experimental set up and model validation

Test bench and system characterisation

The test bench used in this study is shown in Figure 3. It is appropriate for the analysis and design of proportional hydraulic systems. It consists of a hydraulic power and conditioning unit (HPCU), two workstations, a VXI data acquisition system and computers with MATLAB/SIMULINK software installed. At the workstations, different components can be assembled, including asymmetric and symmetric cylinders, asymmetric and symmetric valves, pressure and position transducers and a loading system comprised of springs with different pre-load displacements and spring rates.

The technical specifications and parameters of the hydraulic components used in this study are shown in Table 1. The acronyms SV and AV refer to symmetric and asymmetric valves, respectively, and SC and AC to symmetric and asymmetric cylinders, respectively.

Non-linear dynamic model

Considering Figure 1, the flow rates through an EHV, including the effects of internal leakage as described in Pereira (2007), Destro (2014), and Szpak *et al.* (2010) can be written as:

For $U_c \geq 0$:

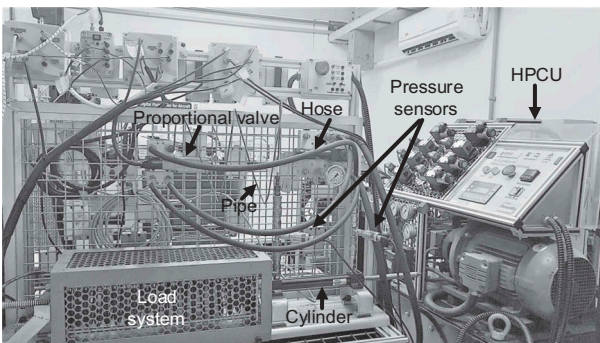


Figure 3. Experimental set up.

Table 1. Parameters of hydraulic components.

HPCU parameters	
Nominal supply pressure	7 MPa (70 bar)
Fluid temperature	40 ± 1 °C
Effective bulk modulus	1.4 × 10 ⁹ Pa
SV – Bosch Rexroth 4WRPEH 6C3B12L	
Orifice area ratio	1
Nominal voltage	± 10 V
Nominal flow rate	12 L/min @ 70 bar
Internal leakage	300 cm ³ /min
Natural frequency	377 rad/s
Damping ratio	0.7
Flow coefficient at port A or B	1.07 × 10 ⁻⁷ m ³ /(s√Pa)
Internal leakage coefficient	7.9 × 10 ⁻¹⁰ m ³ /(s√Pa)
AV – Bosch Rexroth 4WREE 6 E1-08–22	
Orifice area ratio	2
Nominal voltage	± 10 V
Nominal flow rate	8 L/min @ 10 bar
Internal leakage	500 cm ³ /min
Natural frequency	439.8 rad/s
Damping ratio	0.8
Flow coefficient at port A	1.89 × 10 ⁻⁷ m ³ /(s√Pa)
Internal leakage coefficient	3.73 × 10 ⁻¹⁰ m ³ /(s√Pa)
SC – Bosch Rexroth CGT3MS22518200	
Stroke	200 mm
Area chamber A	2.37 × 10 ⁻⁴ m ²
Area chamber B	2.37 × 10 ⁻⁴ m ²
Chamber A initial volume	4.74 × 10 ⁻⁶ m ³
Chamber B initial volume	4.27 × 10 ⁻⁵ m ³
AC – Bosch Rexroth CDT3MS22518200	
Stroke	200 mm
Area chamber A	4.91 × 10 ⁻⁴ m ²
Area chamber B	2.37 × 10 ⁻⁴ m ²
Chamber A initial volume	9.82 × 10 ⁻⁶ m ³
Chamber B initial volume	4.27 × 10 ⁻⁵ m ³

$$qv_A = \left(K_{vA} \frac{U_c}{U_{Cn}} + K_{v_{inA}} \right) \sqrt{p_S - p_A} - K_{v_{inA}} \sqrt{p_A - p_T} \quad (4)$$

$$qv_B = \left(K_{vB} \frac{U_c}{U_{Cn}} + K_{v_{inB}} \right) \sqrt{p_B - p_T} - K_{v_{inB}} \sqrt{p_S - p_B} \quad (5)$$

For $U_c < 0$:

$$qv_A = - \left(K_{vA} \frac{|U_c|}{U_{Cn}} + K_{v_{inA}} \right) \sqrt{p_A - p_T} + K_{v_{inA}} \sqrt{p_S - p_A} \quad (6)$$

$$qv_B = - \left(K_{vB} \frac{|U_c|}{U_{Cn}} + K_{v_{inB}} \right) \sqrt{p_S - p_B} + K_{v_{inB}} \sqrt{p_B - p_T} \quad (7)$$

where qv_A and qv_B represent the flow rates at ports A and B, respectively; p_A and p_B are the pressures in lines A and B, respectively; p_S and p_T represent the supply and the reservoir pressures, respectively; U_{Cn} is the nominal control voltage. K_{vA} and K_{vB} represent the flow coefficients at ports A and B, respectively. Likewise, $K_{v_{inA}}$ and $K_{v_{inB}}$ are the internal leakage coefficients.

The flow coefficient at port A (K_{vA}) can be determined from the nominal flow rate at a pressure drop

measured between two ports (usually P to A) given in the valve catalogue. However, sometimes the manufacturers specify the nominal flow rate at the total pressure drop (P to T) for symmetric valves and the result from Equation (2) must be divided by $\sqrt{2}$ to obtain Kv_A (De Negri *et al.* 2008). The Kv_B value depends on the asymmetry stated in the technical data sheet.

Moreover, the valve internal leakage given by manufacturers corresponds to the maximum flow rate from P to T that occurs at the spool null position and supply pressure of 10 MPa. The test is carried out according to ISO 10770-1 (2009) with ports A and B interconnected. Therefore the internal leakage coefficients cannot be distinguished when using catalogue data and are calculated by:

$$Kv_{inA} = Kv_{inB} = \frac{qv_P}{\sqrt{2}p_S}, \quad (8)$$

where qv_P represents the flow rate at port P and p_S is the supply pressure (pressure at port P).

Applying the continuity equation for each cylinder chamber and assuming the null piston position as retracted at 10% of the stroke, the chamber volumes changing with the piston movement, and no external or internal leakages, yields:

$$qv_A = A_A \frac{dx}{dt} + \frac{V_{A0} + A_A x}{\beta_e} \frac{dp_A}{dt} \quad (9)$$

and

$$qv_B = A_B \frac{dx}{dt} - \frac{V_{B0} - A_B x}{\beta_e} \frac{dp_B}{dt}, \quad (10)$$

where $V_{A0} = 0.1A_AL$ and $V_{B0} = 0.9A_BL$ represent the initial volumes in chambers A and B, respectively; L is the cylinder stroke; x is the piston displacement; and β_e is the effective bulk modulus.

Moreover, applying Newton's second law to the cylinder piston, results in:

$$p_A A_A - p_B A_B = M_t \frac{d^2x}{dt^2} + F_{fr} + \text{sgn}(F_L)|F_L| \quad (11)$$

where M_t is the total mass, F_{fr} is the friction force and F_L the external load force. A positive $\text{sgn}(F_L)$ value corresponds to a compression force.

Moreover, the friction force is expressed by:

$$F_{fr} = f_v \frac{dx}{dt}, \quad (12)$$

where f_v corresponds to the variable viscous friction coefficient (Gomes and Rosa 2003) which is determined for piston velocity ranges as presented in Appendix A.

Non-linear model validation

The equations presented in the previous chapter were implemented in MATLAB/SIMULINK and using a proportional controller. The model validation was carried out by comparison with pressure and displacement signals obtained experimentally using the SV + SC system configuration described in Table 2.

Figure 4 shows the simulation and experimental responses, where it is possible to observe very good match in the steady state; however, some deviation during the transient periods was detected. The maximum differences were 2.6 mm (7.7%) at 2.3 s and 3.5 mm (11.67%) at 4.3 s.

The pressure behaviour in chambers A and B is shown in Figures 4 and 5. The supply and return pressure curves are those measured during the experiment, which were used for simulation purposes. Therefore, the same

Table 2. Parameters of SV+SC configuration.

Valve	4WRPEH 6C3B12L
Cylinder	CGT3MS22518200
Equivalent load mass	28 kg
Supply pressure	70 bar
Reference signal amplitude	50 mm
Reference signal offset	20 mm
Reference signal type	Step
Proportional gain	5

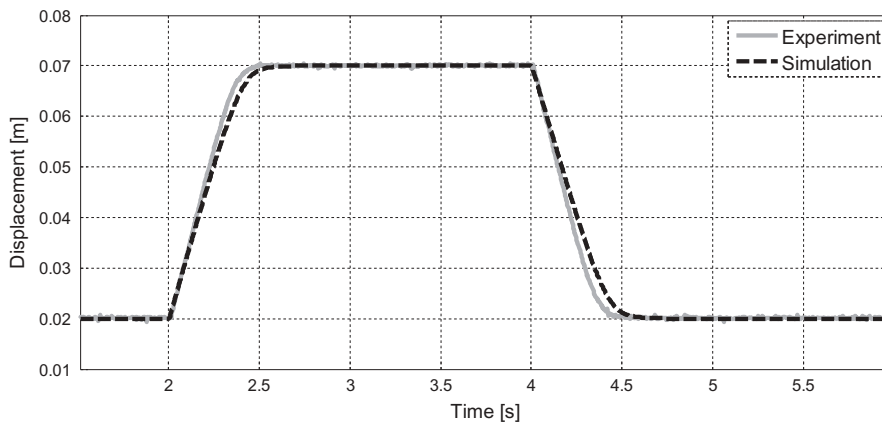


Figure 4. Cylinder displacement.

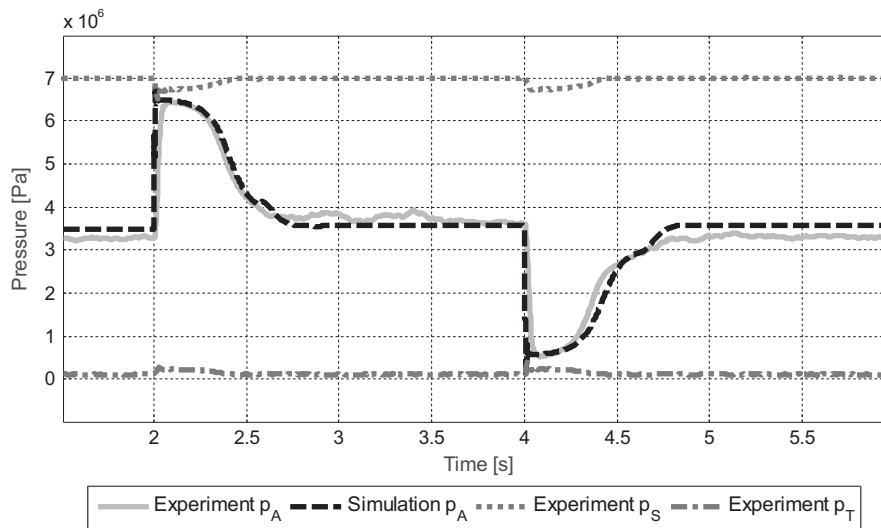


Figure 5. Pressure in cylinder chamber A.

parameters and operating conditions were applied in the experimental set up and the model. The pressure responses show similarity, which verifies the capability of the non-linear model to describe the dynamic effects. After reaching a position, the cylinder oscillates around the steady-state value. This can be seen at the experimental curve in Figure 4, and also in the experimental pressure oscillations reported in Figures 4 and 5. The dominant force in this case is the friction force.

It is important to notice that the pressure in chamber B changes synchronously with pressure A, whereas usually it would be expected the pressures having opposite behaviours. In the experimental set up, a rigid pipe of 1.75 m of length and 2 mm of diameter connecting ports B of the valve and cylinder was used. This pipe introduces fluid acceleration/deceleration and, consequently, it emulates the effect of a moving mass attached to the cylinder rod. However, this strategy introduces also an expressive load loss, resulting on the pressure B behaviour seen in Figure 6. The simulation model

included a load loss coefficient of $5.3 \times 10^{-12} \text{ m}^3/\text{sPa}$ determined experimentally in order to reproduce the dynamic behaviours shown above.

Critical pressure conditions in the cylinder chambers

The main limitation when using an asymmetric cylinder driven by a symmetric valve, or vice-versa, is the occurrence of pressures below zero (negative spikes) or above the supply pressure (positive spikes) in the cylinder chambers.

Using the validated non-linear model, critical pressure conditions were evaluated for different valve and cylinder combinations. As an example, Figure 7 shows the step responses for a SC-AV configuration. The critical conditions occur during the forward movement with maximum negative acceleration and during the return movement with maximum positive acceleration. It is important to notice that cavitation is not predicted by

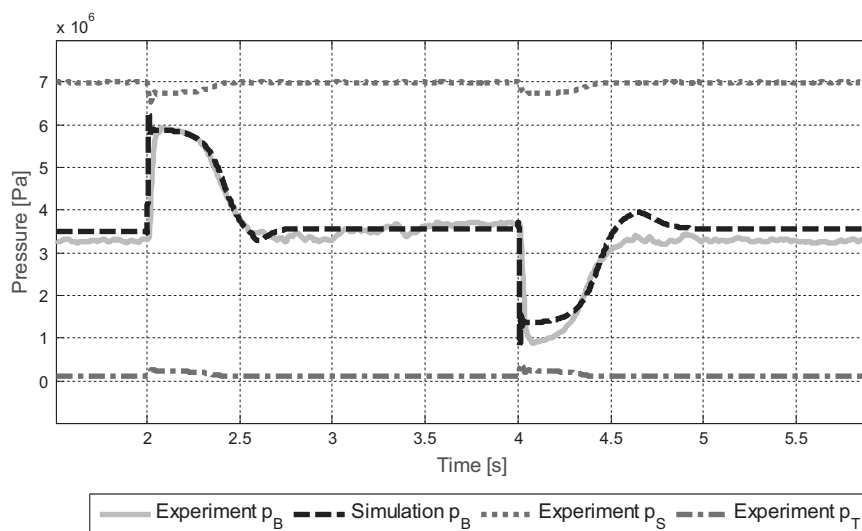


Figure 6. Pressure in cylinder chamber B.

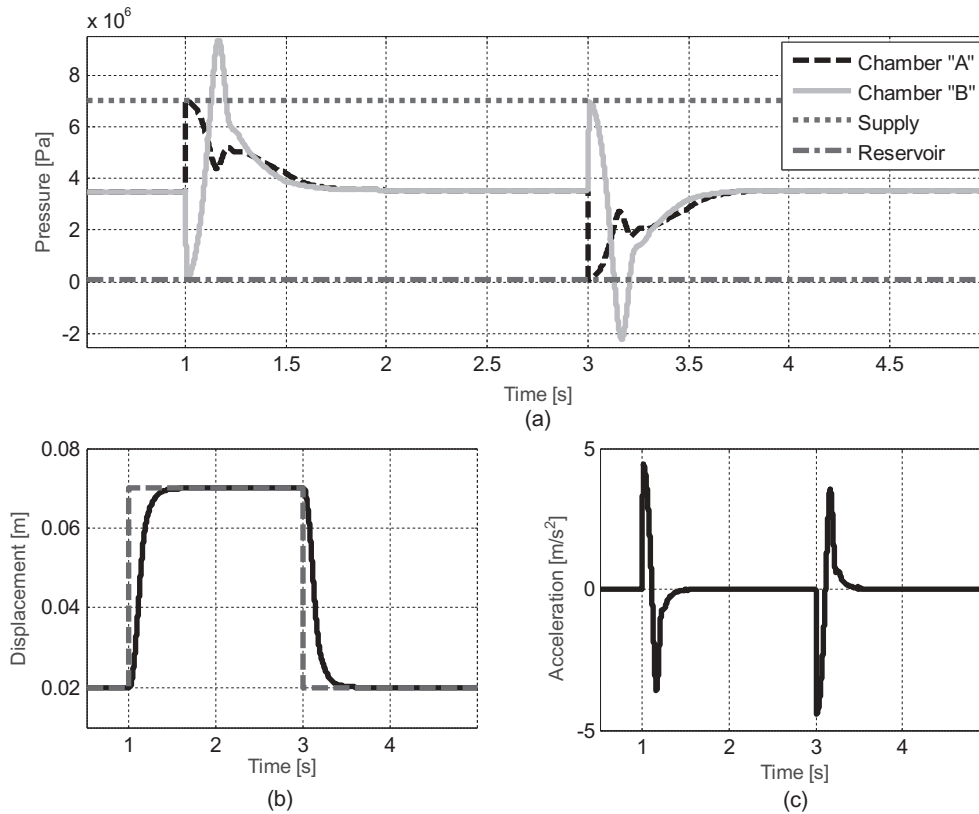


Figure 7. Critical pressure conditions for a SC+AV configuration: (a) cylinder pressures; (b) position; and (c) acceleration.

the model and, consequently, negative pressure values may result from simulations. In real system operation, the pressure inside the chambers will not reach negative values, but there will be a tendency for cavitation due to vaporisation of the fluid and subsequent bubble collapses. Irregular cylinder movement will be expected on that conditions.

Similar results were obtained with the other three system configurations, indicating that critical pressure can occur under the following conditions (Destro 2014):

- (1) On deceleration during forward movement:
 - (1.1) with positive pressure peak (high pressure) in chamber B or;
 - (1.2) with negative pressure peak (low pressure) in chamber A.
- (2) On deceleration during return movement:
 - (2.1) with positive pressure peak (high pressure) in chamber A or;
 - (2.2) with negative pressure peak (low pressure) in chamber B.

According to the simulation results, critical pressure does not occur simultaneously in the two cylinder chambers. Depending on the system configuration and parameters, the pressure peak will be observed either in chamber A or in B.

In order to estimate the influence of the system parameters in a specific valve-cylinder configuration,

simplified equations that can be solved analytically are derived in the next chapter. Using these expressions, a method to help the designer select a valve is presented in a later section.

Analytical model – valve selection

Correlation between r_V and r_A

The flow coefficients (K_{V_A} and K_{V_B}) are usually much higher than the internal leakage coefficients ($K_{V_{inA}}$ and $K_{V_{inB}}$) and thus the effect of valve leakage is only significant when the valve is operating near its null position. However, the critical pressure conditions occur at instants of maximum deceleration, when the valve is opened. Therefore, the terms $K_{V_{inA}}$ and $K_{V_{inB}}$ in Equations (4)–(7) can be neglected in this analysis.

Assuming that the variation of fluid mass associated with the fluid compressibility (Equations (9) and (10)) can be neglected in the following analysis, the flow rate at the cylinder ports can be expressed as the piston area times the velocity. Furthermore, considering the connection between the valve and cylinder shown in Figure 1, when the voltage applied to the valve (U_C) is greater than zero, the piston moves forward. With a negative voltage, the return movement of the piston occurs.

Therefore, taking into account the above simplifications, Equations (4)–(7) can be combined with (9) and (10), yielding:

For $U_C \geq 0$:

$$\frac{dx}{dt} = \frac{\left(Kv_A \frac{U_C}{U_{Cn}}\right) \sqrt{p_S - p_A}}{A_A} \quad (13)$$

$$\frac{dx}{dt} = \frac{\left(Kv_B \frac{U_C}{U_{Cn}}\right) \sqrt{p_B - p_T}}{A_B} \quad (14)$$

For $U_C < 0$:

$$\frac{dx}{dt} = \frac{-\left(Kv_A \frac{|U_C|}{U_{Cn}}\right) \sqrt{p_A - p_T}}{A_A} \quad (15)$$

$$\frac{dx}{dt} = \frac{-\left(Kv_B \frac{|U_C|}{U_{Cn}}\right) \sqrt{p_S - p_B}}{A_B} \quad (16)$$

Combining Equations (13) and (14) for the forward movement and Equations (15) and (16) for the return movement, and including the cylinder area ratio r_A (Equation (1)) and the valve area ratio r_V (Equation (2)), the following relationships between r_A and r_V as a function of the movement direction of the cylinder can be obtained:

For forward movement ($U_C > 0$):

$$r_A = \sqrt{\frac{p_S - p_A}{p_B - p_T}} r_V \quad (17)$$

For return movement ($U_C < 0$):

$$r_A = \sqrt{\frac{p_A - p_T}{p_S - p_B}} r_V \quad (18)$$

According to the previous chapter, the critical pressures occur at maximum deceleration during both the forward and return movements. As discussed in De Negri *et al.* (2008) and Muraro *et al.* (2013), the required performance of a closed-loop positioning system response can be described by a generic second-order time step response. On deriving this expression twice, the maximum accelerations (a_{max}) are obtained. If an underdamped response is expected, the maximum negative acceleration during a forward movement ($x_{step} > 0$) or the maximum positive acceleration during a return movement ($x_{step} < 0$) is expressed by:

$$a_{max} = -x_{step} \omega_{n\ sys}^2 e^{\frac{-2\zeta_{sys}}{\sqrt{1-\zeta_{sys}^2}} \tan^{-1} \frac{\sqrt{1-\zeta_{sys}^2}}{\zeta_{sys}}} \quad (19)$$

where x_{step} is the desired displacement resulting from the step input, $\omega_{n\ sys}$ the natural frequency of the positioning system and ζ_{sys} the damping ratio.

On the other hand, if a critically damped response is expected, the acceleration equation becomes:

$$a_{max} = -x_{step} \omega_{n\ sys}^2 e^{-2} \quad (20)$$

Moreover, p_A and p_B can be considered equal to zero or the supply pressure, that is, the lower and higher admissible pressures, respectively. Assuming these operating conditions, Equations (17) and (18) can

be combined with Equation (11), resulting in the relationships between the r_V and r_A as a function of the load mass, friction and load forces, cylinder areas, and the maximum deceleration. These expressions are presented below, classified according to the piston movement direction.

- Forward movement (FWR) with maximum negative acceleration

(i) Low pressure in chamber A:

$$r'_V = \sqrt{\frac{M_t |a_{max\ n}| - F_{fr} + \text{sgn}(F_L) |F_L| - A_B p_T}{A_B p_S}} r_A \quad (21)$$

(ii) High pressure in chamber B:

$$r''_V = \sqrt{\frac{A_A (p_S - p_T)}{M_t |a_{max\ n}| - F_{fr} + \text{sgn}(F_L) |F_L| + (A_A - A_B) p_S}} r_A \quad (22)$$

- Backward movement (BWRD) with maximum positive acceleration

(iii) Low pressure in chamber B:

$$r'''_V = \sqrt{\frac{A_A p_S}{M_t a_{max\ p} + F_{fr} - \text{sgn}(F_L) |F_L| - A_A p_T}} r_A \quad (23)$$

(iv) High pressure in chamber A:

$$r''''_V = \sqrt{\frac{M_t a_{max\ p} + F_{fr} - \text{sgn}(F_L) |F_L| - (A_A - A_B) p_S}{A_B (p_S - p_T)}} r_A \quad (24)$$

The above equations determine the flow coefficient ratios where critical pressure conditions occur. To obtain Equation (21), p_A was assumed to be equal to zero (minimum pressure) and in Equation (24) p_A was equal to p_S (maximum pressure), resulting in a minimum allowed value of r_V . On the other hand, p_B was substituted by the maximum pressure value (p_S) in Equation (22) and by zero (minimum pressure) in Equation (23), resulting in the maximum allowed value of r_V . The ranges for r_V where the pressures are greater than zero or lower than the supply pressure are summarised in Table 3.

The valve metering area ratio selected must satisfy the criteria associated with chambers A and B simultaneously. For example, during a forward movement, the r_V adopted must be greater than the r_V resulting from Equation (21) and lower than that resulting from Equation (22).

Depending on the system parameters and the expected acceleration, Equations (21) to (24) can result in an imaginary number. In this case, the intended forward or backward movement will not

Table 3. Range of r_V values to avoid critical pressure conditions.

Piston movement	Critical pressure condition	Range of r_V
FWD Neg. accel. BWRD	Low pressure ($p_A = 0$)	Higher than the calculated value
Pos. accel. FWD	High pressure ($p_A = p_S$)	
Neg. accel. BWRD	High pressure ($p_B = p_S$)	
Pos. accel.	Low pressure ($p_B = 0$)	Lower than the calculated value

occur. The feasibility of an operating point can be verified using Equations (17) and (18), resulting in the pressure conditions shown in Table 4.

Analytical model validation

The validation of the calculation of valid ranges for the valve flow coefficient ratios predicted by the Equations (21)–(24) was carried out by dynamic simulation using the validated non-linear model presented above.

The friction force used in the analytical model was 5% of the maximum force exerted by the actuator in the forward movement considering a supply pressure of 70 bar and return pressure of 1 bar. The reference signals were successive steps of 50 mm. The forward movement is from 20 mm to 70 mm at 1 s and the return from 70 mm to 20 mm at 3 s.

In order to change the values of r_V , the value of flow coefficient at port A was assumed to be equal of the valve Bosch Rexroth 4WRPEH 6C3B12L (Table 1) and the flow coefficient at port B was set according to the values of r_V calculated for each condition analysed.

Using a symmetric cylinder, the system characteristics shown in Table 5 were considered. Table 6 shows the results of the r_V calculation carried out with the analytical model for the four critical conditions (Equations (21)–(24)).

The r_V value must be lower than 0.90 and greater than 1.12, resulting in an empty interval, which means that it is impossible to avoid all four critical conditions described in the first column. Moreover, using Equation (18), the corresponding pressure in chamber B (for $p_A = p_S$) is negative and the pressure in chamber A (for $p_B = 0$) is greater than the supply pressure.

In the following paragraphs, the pressure responses of the electro-hydraulic positioning system

for three different configurations are analysed. The non-linear dynamic model, with the parameters shown in Table 5 is used. As mentioned before, the cavitation effect is not predicted by the model and, consequently, the pressures will not reach such high negative values in real operational conditions.

Figure 8 shows the pressure behaviour when using a valve with $r_V = 0.5$. Negative pressure in chamber A during the forward movement and pressure higher than the supply pressure during the return movement are observed. These critical conditions are predicted by the analytical model, since to avoid these negative and positive critical conditions in chamber A, the r_V values should be greater than 0.66 and 1.12, respectively.

On the other hand, the pressure in chamber B does not achieve critical values (Figure 8), as predicted in Table 6. The value of r_V satisfies both conditions: it is lower than 0.90, avoiding pressure below zero and lower than 1.48, avoiding pressure higher than the supply pressure.

Through the dynamic simulation it is possible to note that the pressure in chamber A reaches a peak value much further from the supply pressure than the peak values below the return pressure. This is due to the fact that the r_V value is farther from the optimal r_V condition of the positive peak (difference of 0.62) than that of the negative peak (difference of 0.16).

Figure 9 shows the simulation of the position control system using the symmetric cylinder with a symmetric valve ($r_V = 1$). In this case, a positive peak in chamber A and a negative peak in chamber B occur with the deceleration during the return movement. According to the analytical model, r_V should be greater than 1.12 and lower than 0.90 to avoid critical operational conditions.

Finally, in Figure 10 the behaviour of the pressure cylinder chambers using a valve with $r_V=2$ is shown. In this arrangement, positive and negative peaks occur in chamber B. These two critical conditions can be explained through the analytical model, where the ideal values for the flow coefficient ratio should be lower than 1.48 and 0.90, respectively.

The analysis presented in the above paragraphs exemplifies that the analytical model predicts accurately the occurrence of critical pressure conditions in cylinder chambers without the need to perform a dynamic simulation.

Table 4. Conditions for a valid model response.

Piston movement	Critical pressure condition	Condition for real r_V
FWD Neg. accel. BWRD	Low pressure ($p_A = 0$)	$p_B > p_T$
Pos. accel. FWD	High pressure ($p_A = p_S$)	$p_B < p_S$
Neg. accel. BWRD	High pressure ($p_B = p_S$)	$p_A < p_S$
Pos. accel.	Low pressure ($p_B = 0$)	$p_A > p_T$

Table 5. System characteristics resulting in an unsuitable condition.

Cylinder	CGT3 25/18/200
Forward maximum deceleration	$a_{max n} = -2.3 \text{ m/s}^2$
Backward maximum deceleration	$a_{max p} = 3.4 \text{ m/s}^2$
Friction force	$F_{fr} = 81.7 \text{ N}$
External force (compression)	$F_L = -300 \text{ N}$
Total mass	$M_t = 500 \text{ kg}$

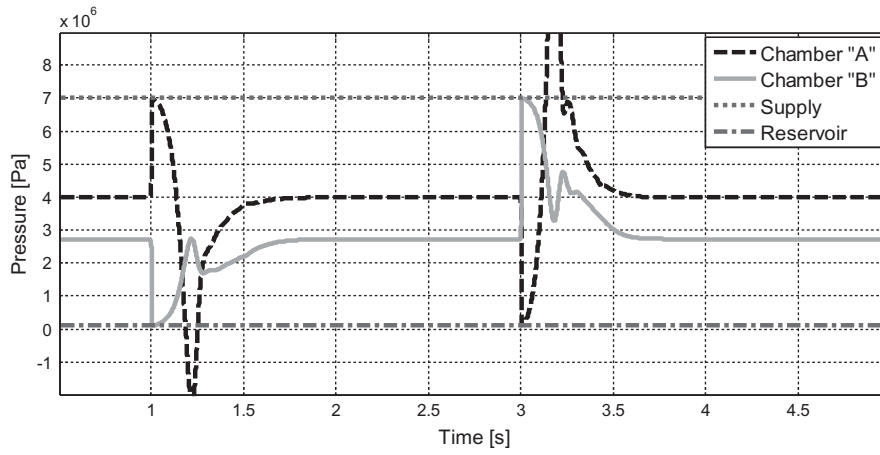


Figure 8. Unsuitable operating condition – symmetric cylinder and valve with $r_V=0.5$.

Table 6. Model response under the unsuitable condition.

Piston movement	Critical condition	Pressure in opposite chamber [Pa]	Range of r_V
FWD Neg. accel.	$p_A = 0$	$p_B = 31.4 \times 10^5$	> 0.66
BWRD Pos. accel.	$p_A = p_s$	$p_B = -17.3 \times 10^5$	> 1.12
FWD Neg accel.	$p_B = p_s$	$p_A = 38.6 \times 10^5$	< 1.48
BWRD Pos. accel.	$p_B = 0$	$p_A = 83.7 \times 10^5$	< 0.90

Choosing a flow coefficient ratio

Considering Equations (21)–(24) and the inequalities described in Table 3, it is possible to determine the eligible values for the valve flow coefficient ratio (r_V) as a function of any operational condition or system parameter present in these equations. The results presented below are based on the system requirements shown in Table 7. The maximum positive and negative accelerations were calculated using Equation (20) for an underdamped response and a desired steady state displacement of 0.08 m and a desired natural frequency of 8.57 rad/s

(corresponding to a settling time of 0.7 s). Considering a supply pressure of 70 bar and return pressure of 1 bar, the maximum hydraulic force is 1635.3 N for the symmetric cylinder and 3413.3 N for the asymmetric cylinder. The friction forces, estimated as 5% of the maximum hydraulic forces, are 81.7 N and 170.7 N, respectively.

Figure 11 shows the r_V value as a function of the load force for the symmetric cylinder. Curve 1 corresponds to Equation (23) and curve 2 to Equation (24) and their intersection at point A determines when the lower pressure in chamber B and higher pressure in chamber A occurs simultaneously. Curve 3 corresponds to Equation (21) and curve 4 to Equation (22) and the intersection at point B corresponds to lower pressure in chamber A and higher pressure in chamber B. Points A and B determine the maximum negative and positive external forces that can be applied, considering the system parameters.

Intersection point C indicates that for a symmetric cylinder with load force around zero, lower pressure in chamber B will occur with the maximum

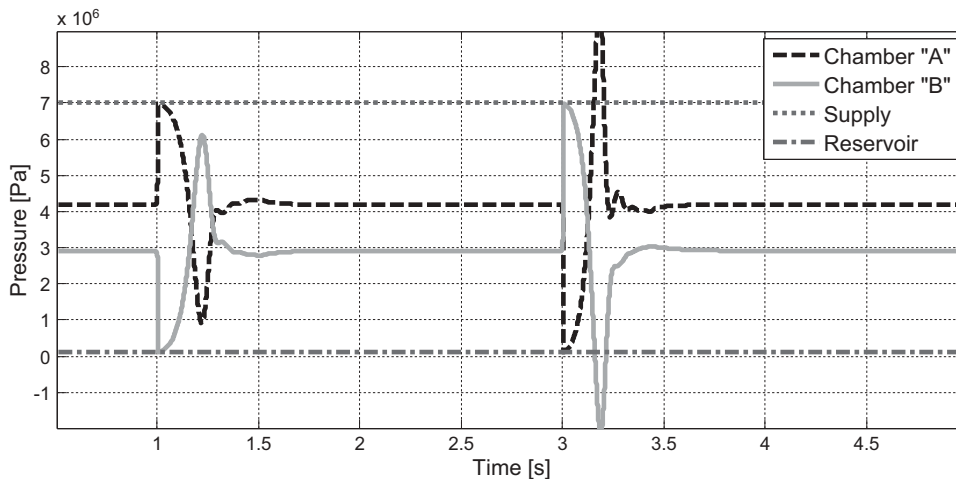


Figure 9. Unsuitable operating condition – symmetric cylinder and valve with $r_V=1$.

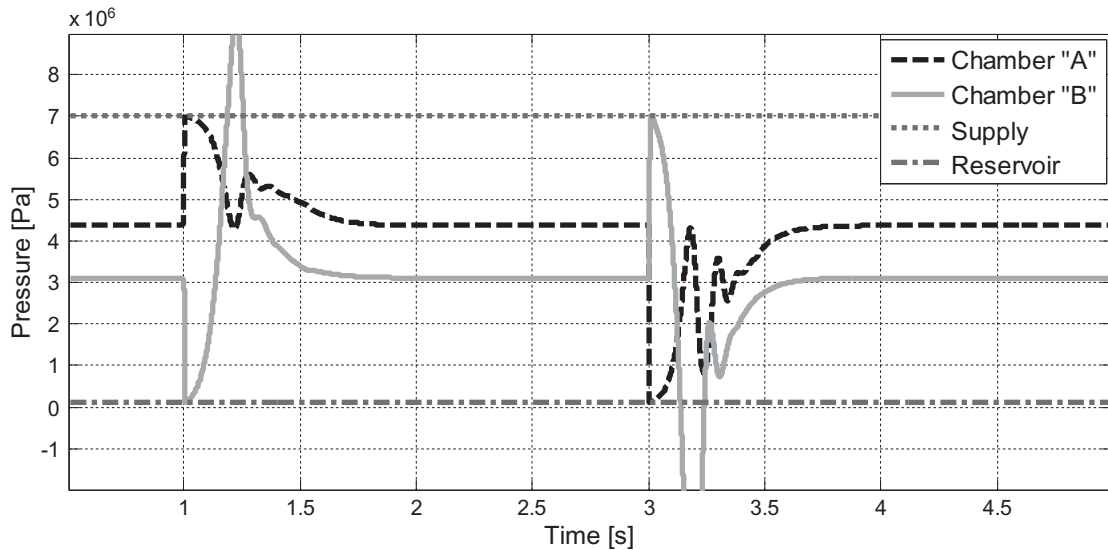


Figure 10. Unsuitable operating condition – symmetric cylinder and valve with $r_v=2$.

Table 7. System requirements to obtain the static model response.

Symmetric cylinder	CGT3 25/18/200
Asymmetric cylinder	CDT3 25/18/200
Steady state displacement	80 mm
Settling time	700 ms
Damping ratio	1.0
Forward maximum deceleration	$a_{max n} = -0.8 \text{ m/s}^2$
Backward maximum deceleration	$a_{max p} = 0.8 \text{ m/s}^2$
Total mass	$M_t = 100 \text{ kg}$

acceleration during the backward movement and higher pressure in this chamber will occur during the forward movement. Point D corresponds to the higher and lower pressures in chamber A during the backward and forward movements, respectively. With load force equal zero, the wider range of eligible r_v values can be noted.

The area delimited by curves 1 to 4 defines the working region for the hydraulic system. As expected,

a symmetric valve provides a match with a symmetric cylinder for any external load.

When convenient, it is possible to estimate the maximum positive or negative deceleration or load force by equalising Equations (23) and (24) and Equations (21) and (22).

In Figure 12, the chart shows the flow coefficient ratio versus load force for the asymmetric cylinder (Table 7). Due to the cylinder asymmetry, the working area is shifted to the left compared with Figure 11. Since there is no rod on cylinder side A, the corresponding area is greater and, consequently, the working limit with external compression forces is higher. The area of chamber B is unchanged and thus the working limit for traction forces (point B) is similar to obtained in Figure 11.

A flow coefficient ratio of 2, corresponding to the cylinder area ratio, is adequate for the whole range of

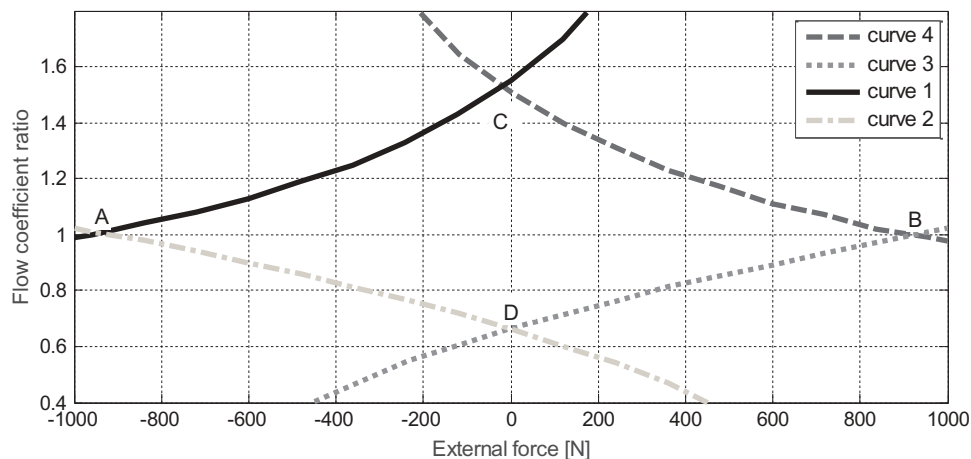


Figure 11. Influence of external force on the electro-hydraulic positioning system using a symmetric cylinder.

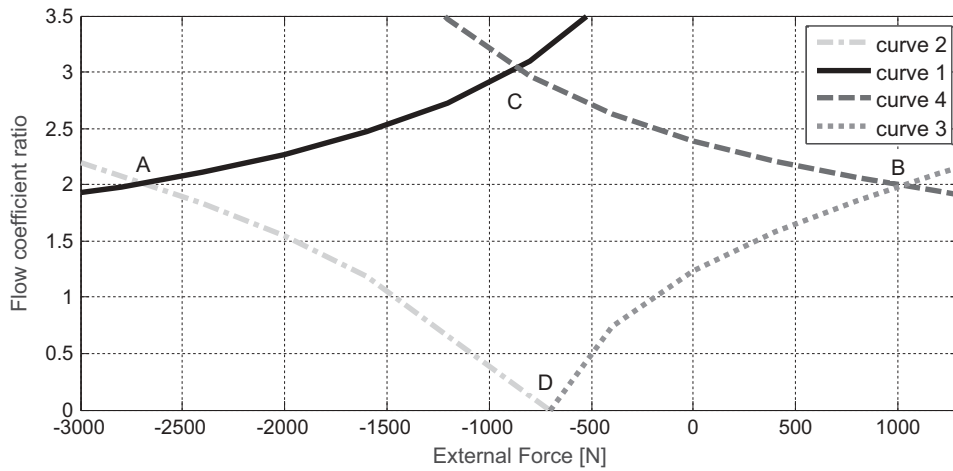


Figure 12. Influence of external forces on the electro-hydraulic positioning system using an asymmetric cylinder.

forces. However, even a symmetric valve can be used in this case. This explains why several practical hydraulic systems use an asymmetric cylinder with a symmetric valve and achieve good performance without cavitation or overpressure.

Method for choosing a flow coefficient ratio

A general procedure for predicting the range of valve flow coefficients suitable for a specific application can be derived from the equations and analysis presented in this paper. As discussed in before, critical pressure

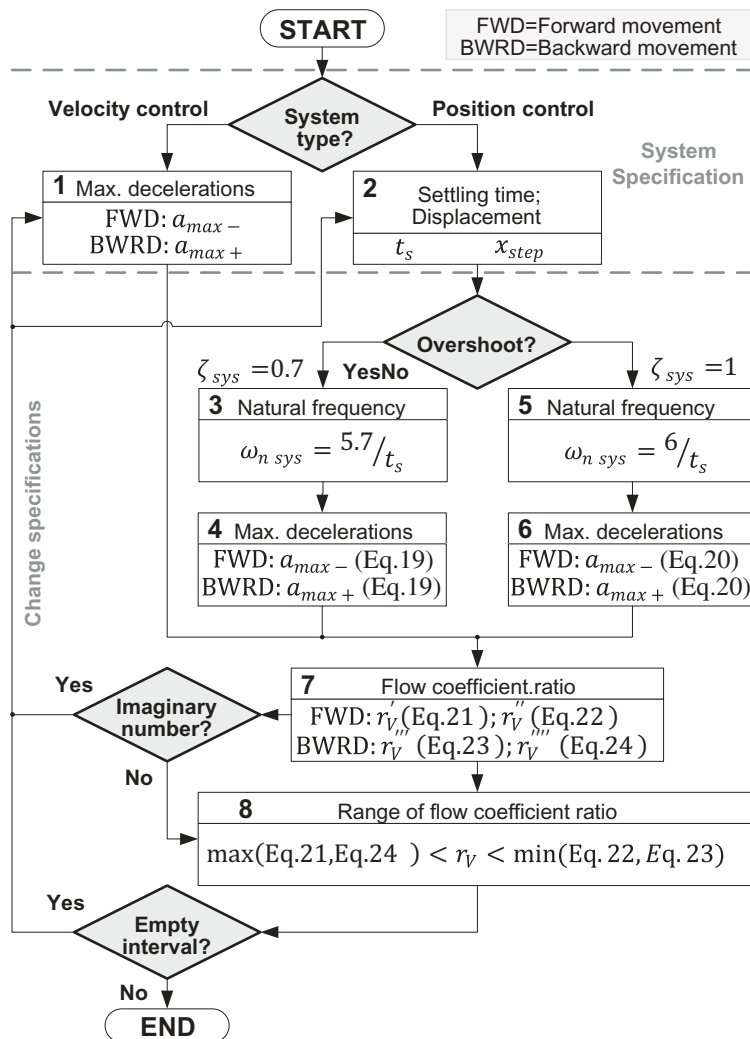


Figure 13. Method for choosing a flow coefficient ratio.

conditions can occur during the piston deceleration. This statement is valid for open or closed-loop systems controlled by a valve.

The required system parameters are the load force, moved mass and friction force. In case of an unknown cylinder friction, this can be estimated as 10% of the maximum hydraulic force. The cylinder areas must be determined previously.

According to the flow chart shown in Figure 13, in the case of a velocity control system (open or closed loop), the maximum desired deceleration in both movement directions must be specified. For position control systems, the maximum decelerations are derived from Equations (19) or (20), depending on the type of the response expected, where the desired displacement and the settling time are introduced.

Based on these specifications and preliminary calculations, four values for the flow coefficient ratio must be determined using Equations (21)–(24). If some of these equations result in the square root of a negative number, the system specifications must be modified. The system specifications must also be modified if the result is an empty interval.

Considering that the external load force and moved mass are related to the application, the deceleration is the system requirement that can usually be relaxed.

Conclusions

The dimensioning of electro-hydraulic positioning systems was discussed in this paper, focusing on the combination of symmetric and asymmetric cylinders with symmetric and asymmetric valves. Based on the system modelling at the maximum negative and positive accelerations, a set of equations was proposed for determining the range of the valve flow coefficient ratio in which critical pressures will not occur in the cylinder chambers.

A validated non-linear dynamic model was used to verify the accuracy of the analytical model. Estimates of the occurrence of pressure peaks as well as normal operation conditions were verified by comparing results obtained from the dynamic model and the simplified equations, demonstrating the applicability of the proposed approach.

The selection of the electro-hydraulic positioning system configuration using the proposed model requires only basic system parameters including moved mass, estimated friction force and load force. The maximum deceleration in the forward and backward movement must also be quantified

based on the desired dynamic response of the system. Assuming a cylinder area ratio (r_A) is determined previously, a range for the selection of the valve control orifice area ratio (r_V) is determined. Although the valve and cylinder configuration that best fits the load variations is that of equal ratios ($r_V = r_A$), several other acceptable non-matching configurations can be used.

A method for calculating r_V , which is valid for position control systems as well as for speed control systems, is presented in a flow chart. This method can be used in the preliminary phase of a system design. The valve size can then be determined and, if necessary, a dynamic analysis based on a non-linear model can be performed.

Nomenclature

a_{\max}	Piston maximum acceleration	[m/s ²]
$a_{\max n}$	Piston maximum negative acceleration	[m/s ²]
$a_{\max p}$	Piston maximum positive acceleration	[m/s ²]
A_A	Area of cylinder chamber A	[m ²]
A_B	Area of cylinder chamber B	[m ²]
C_d	Discharge coefficient	[1]
C_{ni}	Polynomial coefficients	[Ns ² /m ²]
C_{pi}	Polynomial coefficients	[Ns ² /m ²]
F_{fr}	Friction force	[N]
F_L	Load force	[N]
f_v	Variable viscous friction coefficient	[Ns/m]
F_{Sp}	Maximum positive static friction	[N]
F_{Sn}	Maximum negative static friction	[N]
K_p	Proportional gain	[1]
K_V	Flow coefficient	[m ³ /(sPa ^{1/2})]
K_{VA}	Flow coefficient at port A	[m ³ /(sPa ^{1/2})]
K_{VB}	Flow coefficient at port B	[m ³ /(sPa ^{1/2})]
$K_{V_{inA}}$	Internal leakage coefficient at port A	[m ³ /(sPa ^{1/2})]
$K_{V_{inB}}$	Internal leakage coefficient at port B	[m ³ /(sPa ^{1/2})]
M_t	Total mass	[kg]
p_A	Pressure in chamber A	[Pa]
p_B	Pressure in chamber B	[Pa]
p_S	Supply pressure	[Pa]
p_T	Return pressure	[Pa]
q_{VA}	Flow rate at port A	[m ³ /s]
q_{VB}	Flow rate at port B	[m ³ /s]
q_{Vn}	Nominal flow rate	[m ³ /s]
q_{VP}	Flow rate at port P	[m ³ /s]
r_A	Cylinder area ratio	[1]
r_V	Valve flow coefficient ratio	[1]
$t_{s\ sys}$	System settling time	[s]
U_c	Valve control voltage	[V]
U_{cn}	Valve nominal control voltage	[V]
U_c	Reference position (voltage)	[V]
U_s	Piston position (voltage)	[V]
v	Piston velocity	[m/s]
$v_{Lim\ n}$	Negative limit velocity	[m/s]
$v_{Lim\ p}$	Positive limit velocity	[m/s]
v_{0n}	Negative stick velocity	[m/s]
v_{0p}	Positive stick velocity	[m/s]
V_{A0}	Initial volume in chamber A	[m ³]
V_{B0}	Initial volume in chamber B	[m ³]
x	Piston displacement	[m]
x_{step}	Desired piston displacement	[m]
w	Orifice width	[m]
β_e	Effective fluid bulk modulus	[Pa]
Δp_n	Nominal pressure drop	[Pa]
ρ	Fluid density	[kg/m ³]
$\omega_n\ sys$	System natural frequency	[rad/s]
ζ_{sys}	System damping ratio	[1]

Disclosure statement

No potential conflict of interest was reported by the authors.

Funding

This work was supported by the CNPq (the Brazilian National Council for Scientific and Technological Development)

Notes on contributors



Thermophysics at UFSC.

Mário C. Destro received his Master in Mechanical Engineering in the field of Mechanical Design Systems with emphasis on Hydraulic and Pneumatic Systems, at Federal University of Santa Catarina (UFSC). At the moment, he is PHD student in the field of hydraulic systems at the POLO-Research Laboratories for Emerging Technologies in Cooling and



Associate Editor of the IJFP and JBSMSE. His research areas include the analysis and design of hydraulic and pneumatic systems and design methodology for mechatronic systems.

Victor J. de Negri has been Head of the Laboratory of Hydraulic and Pneumatic Systems (LASHIP) at the Department of Mechanical Engineering, Federal University of Santa Catarina (UFSC), Brazil, since 1995. He received his D. Eng. degree in 1996 from UFSC. He is a member of ASME and ABCM and

ORCID

Victor J. De Negri  <http://orcid.org/0000-0002-1860-3104>

References

- Asaff, Y., De Negri, V.J., and Soares, J.M.C., 2015. Pneutronic speed governor for small hydropower plants: a new application for pneumatics. *Journal of the Brazilian Society of Mechanical Sciences and Engineering*, 38, 2621–2633. doi:10.1007/s40430-015-0392-7
- De Negri, V.J., Ramos Filho, J.R.B., and Souza, A.D.C., 2008. A design method for hydraulic positioning systems. In: 51th National Conference on Fluid Power (NCFP), Las Vegas, USA: NFPA, 669–679.
- Destro, M.C., 2014. Análise de condições operacionais críticas em posicionadores eletro-hidráulicos (in Portuguese). Thesis (Master's). Federal University of Santa Catarina. Florianópolis, Brazil.
- Detiček, E. and Župerl, U., 2011. An Intelligent Electro-Hydraulic Servo Drive Positioning. *Strojniški vestnik – Journal of Mechanical Engineering*, 57 (5), 394–404. DOI:10.5545/sv-jme.2010.081.
- Furst, F.L., 2001. Sistematização do projeto preliminar de circuitos hidráulicos com controle de posição (in Portuguese). Thesis (Master's), Federal University of Santa Catarina, Florianópolis, Brazil.
- Gomes, S.C.P. and Rosa, V.S., 2003. A new approach to compensate friction in robotic actuators. In: Proceedings of the International Conference on Robotics and Automation, Taipei, Taiwan, Vol. 1, pp. 622–627.
- Guo, J.-C., et al., 2014. Research on Pressure Jump Characteristics of Valve Controlled Asymmetric Cylinder System. *Research Journal of Applied Sciences, Engineering and Technology*, 7 (12), 2469–2474. doi:10.19026/rjaset.7.554.
- ISO 10770-1, 2009. *Hydraulic fluid power — electrically modulated hydraulic control valves — part 1: test methods for four-port directional flow-control valves*. Switzerland: International Organization for Standardization.
- Johnson, J.L., 1996. *Design of Electrohydraulic Systems for Industrial Motion Control*. 2nd. Milwaukee: Parker Hannifin Corporation.
- Kim, M.Y. and Lee, C., 2006. An Experiment Study on the Optimization of Controller Gains for an Electrohydraulic Servo System Using Evolution Strategies. *Control Engineering Practice*, 14, 137–147. doi:10.1016/j.conengprac.2005.01.010
- Lei, J.-B., et al., 2010. Position Control for Asymmetrical Hydraulic Cylinder System Using a Single On/Off Valve. *Journal Shanghai Jiaotong University (Sci.)*, Springer Verlag, 15 (6), 651–656. doi:10.1007/s12204-010-1063-6.
- Muraro, I., Teixeira, P.L., and De Negri, V.J., 2013. Effect of proportional valves and cylinders on the behavior of hydraulic positioning systems. In: *ASME/BATH 2013 Symposium on Fluid Power & Motion Control*, 2013, Sarasota, FL. Bath: ASME, 1–9.
- Pereira, P.I.I., Guenther, R., and De Negri, V.J., 2007. Tracking Control in Hydraulic Actuators Using Slow Proportional Directional Valves. In: 19th International Congress of Mechanical Engineering – COBEM. Rio de Janeiro: ABCM.
- Saad, J. and Liermann, M., 2015. Improved sizing of hydraulic servodrives through inverse simulation approach using Modelica and modified OpenHydraulics library. *International Journal of Fluid Power*, 16 (3), 163–177. doi:10.1080/14399776.2015.1107386
- Sun, P., Grácio, J.J., and Ferreira, J.A., 2006. Control System of a Mini Hydraulic Press for Evaluating Springback in Sheet Metal Forming. *Journal of Materials Processing Technology*. doi:10.1016/j.jmatprotec.2006.02.009
- Szpak, R., Ramos Filho, J.R.B., and De Negri, V.J., 2010. Theoretical and experimental study of the matching between proportional valves and symmetric and asymmetric cylinders In: 7th International Fluid Power Conference – 7 IFK, 2010, Aachen-Germany. Aachen: IFAS, 2010, v 2, 155–166.
- Viersma, T.J., 1980. *Analysis synthesis and design of hydraulic servo systems and pipelines*. New York: Elsevier Scientific Publishing Company.

Appendix A

As mentioned before, the cylinder friction forces were modelled using the variable viscous friction coefficient (f_v) (Equation (12)). This model represents the friction through four different trajectories. Trajectory A corresponds to the friction force described by friction-velocity maps experimentally determined. For piston velocities lower than the minimal experimental value, friction force is represented by either trajectories B (slip mode) or C and D (stick mode) (Gomes and Rosa 2003, Asaff *et al.* 2015).

Therefore, the variable viscous friction coefficient is calculated by:

Trajectory A:

$$f_v = \begin{cases} \sum_{i=0}^k c_{ni} \cdot v^i \text{ for } v \leq v_{Lim\ n} \\ \sum_{i=0}^k c_{pi} \cdot v^i \text{ for } v \geq v_{Lim\ p} \end{cases} \quad (26)$$

Trajectory B:

$$f_v = \begin{cases} \frac{F_{S\ n}}{v_{Lim\ n}} \text{ for } v > v_{Lim\ n} \\ \frac{F_{S\ p}}{v_{Lim\ p}} \text{ for } v < v_{Lim\ p} \end{cases} \quad (27)$$

Trajectory C:

$$f_v = \begin{cases} \frac{F_{S\ n}}{v_{0\ n}} \text{ for } v_{0\ n} \leq v \leq 0 \\ \frac{F_{S\ p}}{v_{0\ p}} \text{ for } 0 < v \leq v_{0\ p} \end{cases} \quad (28)$$

Trajectory D:

$$f_v = \begin{cases} \frac{F_{S\ n}}{v} \text{ for } v_{Lim\ n} < v < v_{0\ n} \\ \frac{F_{S\ p}}{v} \text{ for } v_{0\ p} < v < v_{Lim\ p} \end{cases} \quad (29)$$

The polynomial coefficients and velocity limits for the cylinders used in this paper are presented in Table 8 and Table 9.

Table 8. Friction parameters for cylinder CGT3MS22518200.

Polynomial coefficients	
C_{ni}	$[0.4040, -1.5314, 2.2225, -1.5405, 0.5502, -0.0647, 0.0083] \times 10^4$
C_{pi}	$[-0.4083, -1.5245, -2.2067, -1.5466, -0.5594, -0.0664, -0.0087] \times 10^4$
Parameter	Value
F_{Sp} (maximum positive static friction)	101.65 N
F_{Sn} (minimum negative static friction)	-99.29 N
v_{Limp} (positive limit velocity)	0.0035 m/s
v_{Limn} (negative limit velocity)	-0.0035 m/s
v_{0p} (positive stick velocity)	0.0033 m/s
v_{0n} (negative stick velocity)	-0.0033 m/s

Table 9. Friction parameters for cylinder CDT3MS22518200.

Polynomial coefficients	
C_{ni}	$[9.3322, -1.2358, 0.1489] \times 10^3$
C_{pi}	$[-1.0580, -0.1668, -0.0233] \times 10^4$
Parameter	Value
F_{Sp} (maximum positive static friction)	296.35 N
F_{Sn} (minimum negative static friction)	-232.64 N
v_{Limp} (positive limit velocity)	0.00432 m/s
v_{Limn} (negative limit velocity)	-0.00185 m/s
v_{0p} (positive stick velocity)	0.00410 m/s
v_{0n} (negative stick velocity)	-0.00176 m/s